TÜBİTAK

Turkish Journal of Engineering & Environmental Sciences

http://journals.tubitak.gov.tr/engineering/

Research Article

Turkish J Eng Env Sci
(2013) 37: 79 – 90

doi:10.3906/muh-1203-11

Effect of soil properties on stability of soil–steel culverts

Mehdi Hosseinzadeh SUTUBADI, Behnam Rahrou KHATIBI*
Department of Civil Engineering, University of Tabriz, Tabriz, Iran

Received: 12.03.2012 • **Accepted:** 26.12.2012 • **Published Online:** 04.03.2013 • **Printed:** 01.04.2013

Abstract: Soil–steel structures have been used as an alternative to short span concrete and steel bridges for years because they have some advantages regarding their construction methods, maintenance costs, and construction time. Several researchers have performed experimental and numerical studies about the behavior of these structures under dead loads and crossing live loads. In this study, to investigate the variations of soil properties on the stability of a culvert, we tried to simulate a soil–steel culvert in the PLAXIS program, which is a 2D finite element code for soil and rock analyses. The Mohr–Coulomb constitutive model was used in this simulation, and as the crossing traffic load, the stage construction method was established. Parametric analyses showed that as cohesion (c), Young's modulus (E), and the internal friction angle (φ) increase, the stability of the soil–steel culvert increases. Furthermore, analyses showed that an increase in other properties, such as Poisson's ratio (υ) and the dilation angle (ψ), has a negligible effect on the stability of the soil–steel culvert.

Key words: Soil–steel culvert, PLAXIS, finite element program, soil properties, Mohr–Coulomb constitutive model

1. Introduction

Soil–steel culvers are special structures that have been used for various purposes. These structures are often used as an alternative to short span concrete and steel bridges. A soil–steel culvert consists of a metal crust, whose shape might be classified as a closed section or an open section, and soil backfill that covers the metal crust. Generally, the crust of a culvert is made of either aluminum or steel and its profile shape is corrugated. These corrugated plates are assembled at the site according to relevant designs and plans.

Culverts have several advantages over other structures with the same function. In general, culverts are used as a substitute for bridges with a short-span on temporary and permanent roads. The main advantage of these structures is the savings in the materials used. The short construction time of these structures is another advantage of culverts. Using aluminum or galvanized steel, the probability of erosion and rusting of the metal part of the structure becomes negligible and the maintenance costs of the culvert decrease significantly, and the lifetime of this structure compared to other sorts of structures with the same function is considerably longer.

Because of the several advantages mentioned above, soil–steel structures have been built for many years. These structures have a complex behavior under service loadings; therefore, engineers use traditionally conservative correlations for designing these structures. In the recent years, laboratory testing and numerical simulations have helped researchers to understand the soil–steel structure's behavior and interactions between the soil and steel. Seed and Raines (1988) modeled the failure of a long-span metal culvert during construction under a remarkable live load. Using elastic behavior and a nonlinear elastic behavior for the culvert material, Seed and

*Correspondence: behnam.rahro@gmail.com

Raines (1988) performed a 2D finite element analysis. Byrne et al. (1993) performed an experimental study on the Elkhart Creek culvert, followed by a nonlinear finite element analysis. Experimental measurements were compared with the numerical results. Using the Abaqus program, Girges and Abdel-Sayed (1995) performed 2D and 3D finite element analyses to examine the behavior of soil–steel culverts. As a constitutive model for the soil mass, elastic and extended elastic–plastic Drucker–Prager models were used. Taleb and Moore (1999) conducted 2D and 3D analyses to simulate the behavior of long-span shallow corrugated metal culverts under crossing live loads and during backfilling. The results of this modeling were used as a basis for the American design code (AASHTO) for culvert designing. Barkhordari and Abdel-Sayed (2001) performed a numerical modeling about culvert behavior under loading. In their work, the maximum bearing capacity of a soil–steel culvert and the expansion and sequence of plastic hinges and plastic moments were presented. Several normal and tangential springs were modeled around the culvert shell for modeling normal and shear stresses between the soil mass and metal shell. El-Sawy (2003) performed a 3D finite element analysis for the Deux Rivières culvert, which was built in Ontario, Canada. This model was based on the orthotropic shell theory, in which the stiffness of a corrugated plate varies depending on its orientation. The Deux Rivières culvert was examined by several researchers, such as Bakht (1981) and Moore and Brachman (1994). Machelski and Antoniszyn (2005) carried out a 3D finite element analysis for a long-span culvert. Considering the effect of the metal shell, 2 different models were simulated. The soil–steel interaction was modeled by several elastic springs. Using the finite element program COSMOS, Kunecki (2006) carried out a 3D finite element analysis for a corrugated long-span metal culvert and a laboratory test of this model. Both elastic–plastic and elastic constitutive models were used for the soil mass and steel plates, respectively.

2. Aim and scope

As mentioned in Section 1, several numerical and experimental studies on the behavior of the soil–steel culverts under static and crossing loadings have been conducted so far. Almost all of these studies have investigated soil–steel interactions and the behavior of the culverts under loadings In this study, we tried to examine effects of variations of the soil properties on the stability of a soil–steel culvert using laboratory data and in situ tests, while classifying them in a standard range. For this aim, the 2D finite element program PLAXIS was used, along with a Mohr–Coulomb model as a constitutive model. In this finite element model, the characteristics of the Deux Rivières culvert, situated in Ontario, Canada, were used. As in studies performed by El-Sawy (2003), the orthotropic shell theory was used. The stage construction method was established for applying the crossing loads, which represent the load applied by a truck, to investigate both the loading and unloading effects on the behavior of the culvert structure. Finally, as a parametric study, variations of the soil properties, such as cohesion (c), Young's modulus (E), internal friction angle (φ), Poisson's ratio (υ), and dilation angle (ψ) under crossing load, are discussed.

3. Definition of the soil–steel culvert properties

3.1. Soil properties for the soil–steel culvert modeling

A soil mass, according to its classification, can show different behaviors under various loading conditions. Each constitutive model defined for the soil mass has its own parameters for calculation of deformations and stresses in the soil mass due to external loadings. As used in this study, for example, the Mohr–Coulomb model has some parameters such as E_s, c, φ, υ_s, and ψ, and variation in each of them can cause changes in the stress–strain behavior of the soil mass. In this work, considering the effect of the soil property variations on the stability of

a culvert structure, we tried to collect and analyze some soil properties obtained in the laboratory and from in situ tests of soil samples from several projects. For this aim, 2 sources of data were obtained from operational and research projects. The first data source was a laboratory test performed on the soil samples obtained from a project for bridge construction in Tabriz, Iran. The second data source was several road building projects performed by the Technical and Soil Mechanics Laboratory Co. (tied to the Road and Transportation Ministry of Iran). These data were compared with the soil properties used in the studies by Moore and Brachman (1994) and El-Sawy (2003), and finally, according to Table 1, the upper and lower values were proposed for the parameters needed for the Mohr–Coulomb constitutive model.

Table 1. Upper and lower values of the soil properties used in the finite element modeling and their increments.

Parameter	Unit	Lower value	Upper value	Increment
Cohesion (c)	MPa	10	80	5
Young's modulus (E)	MPa	30	90	10
Friction angle (φ)	Degrees	26	40	2
Poisson's ratio (υ)	-	0.2	0.4	0.05
Dilation angle (ψ)	Degrees	0	3	1

3.2. Mechanical and physical properties of the steel plates used in the soil–steel culvert modeling

As mentioned in Section 2, the characteristics of the Deux Rivières culvert, situated in Ontario, Canada, were used. Previously, researchers such as Bakht (1981), Moore and Brachman (1994), and El-Sawy (2003) performed some studies on this culvert. Figure 1 shows the dimensions and properties of the Deux Rivières culvert. The cross-section of the culvert is circular, with a 7.77-m diameter, and the length of the culvert is 31 m. The metal plates used in the culvert are 5-gauge corrugated steel plates, with a thickness of 5.45 mm and a plate pitch and depth of 152 mm and 51 mm, respectively. The height of the soil mass on the steel structure is 2.6 m in the centerline of the longitudinal section, which equals one-third of the culvert diameter or span (which is greater than one-sixth of the span). Therefore, this culvert is a deep-buried culvert (AASHTO, 1989).

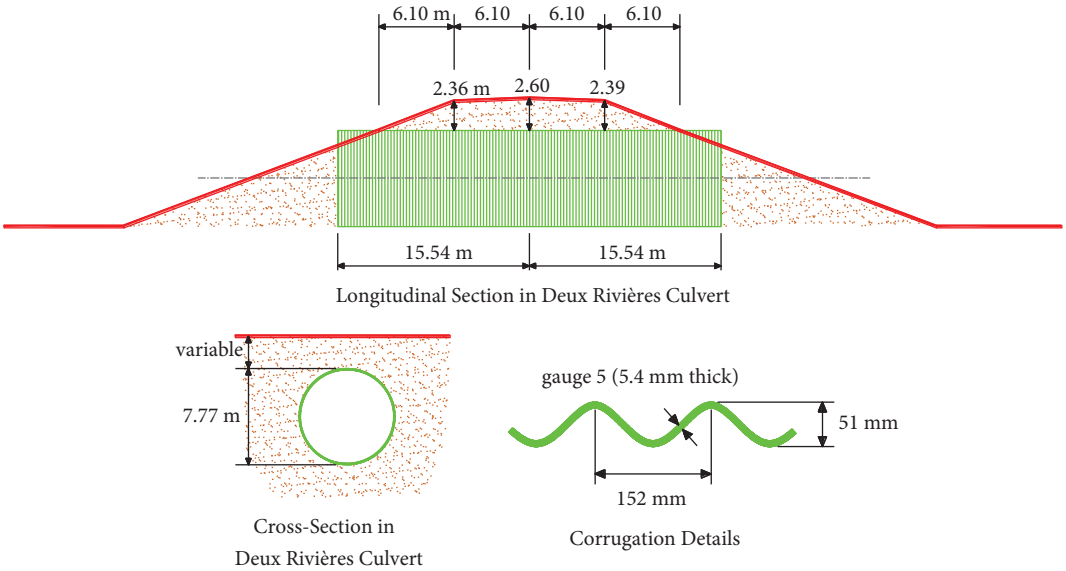

Figure 1. Dimensions and properties of the Deux Rivières culvert (taken from Bakht (1981)).

In the corrugated steel plates, the axial and bending stiffness along both the strong and weak axes are different. According to El-Sawy (2003), these corrugated steel plates can be replaced with an equivalent plate section using Eqs. (1) and (2).

$$\bar{t}=\sqrt{12I/A}=6.1 \text{ mm} \tag{1}$$

$$\bar{E}=12EI/(\bar{t})^3=23080 \text{ MPa} \tag{2}$$

Here, A, E, and I are the area per unit length of the corrugated plate, Young's modulus, and the moment of inertia per unit length of a corrugated plate, respectively. These equations provide the corrugated steel plate to be replaced with a uniform shell.

The properties used in the computer modeling for the metal plates are according to the above-mentioned equations, based on the orthotropic shell theory represented by El-Sawy (2003).

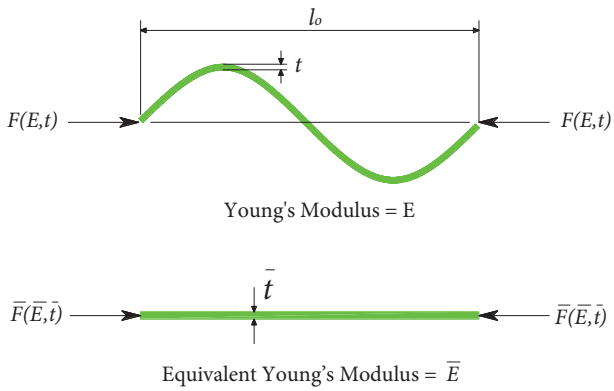

Figure 2. Cross-section of the corrugated plate and its equivalent plate section (taken from El-Sawy (2003)).

4. An introduction to the software and modeling procedure

Choosing appropriate software for the modeling of a soil–steel culvert was one of the most important procedures in this study. Several items have been considered in this way:

1) For the numerical modeling of corrugated metal plates, the software should have proper options to introduce the plate parameters (e.g., span and rise of the culvert, buried depth, E, υ, I, A, ρ, and w).

2) The software should have proper constitutive models or some options to define models needed for the soil mass.

3) The soil–steel interaction effect is an important factor in this study, and so the software should have proper options for this aim.

Considering these items and other conditions, the finite element PLAXIS software was used. There are several constitutive models in PLAXIS, including the Mohr–Coulomb model, hardening-soil model, soft-soil-creep model, soft-soil model, and modified Cam-clay model. These models can be used as a representative for the soil mass, while the model parameters are used as quantifiers for the soil behavior.

The elastic–plastic Mohr–Coulomb constitutive model that was used in this study includes 5 parameters: E and υ for soil elasticity, φ and c for soil plasticity, and ψ as a dilation angle. These parameters, familiar to most geotechnical engineers, can be obtained from basic tests on soil samples. Using the Mohr–Coulomb constitutive model, both elastic and plastic deformations of a soil mass can be calculated.

4.1. Definition of a soil–steel culvert

Figure 3 shows a general cross-section of the soil–steel culvert and stage construction loading method. For the soil profile, 2 separate regions of 20 m in length were defined for the model. The lower layer of the soil profile, named "base soil", was considered as a well-compacted layer according to the AASHTO code and was marked by a light green color. The height of this layer was assumed to be 0.7 m. The main section of the soil profile in the soil mass surrounding the steel structure was named "soil" in the model, with a height of 10 m, and was marked by a pink color.

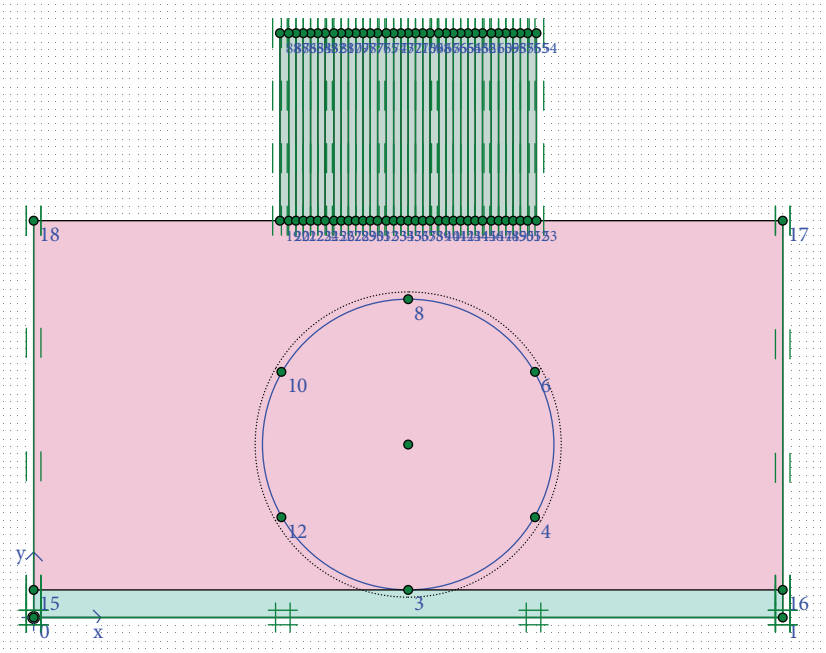

Figure 3. General cross-section of the soil–steel culvert defined for the model.

The steel structure of the culvert was defined within the "soil" layer with the coordinates x = 10 and y = 4.6 and a 7.78-m diameter. Because this metal shell would be surrounded by the "soil" layer, the option of "add interfaces to all sections" was chosen in the program.

The upper part of Figure 3 was assumed for the stage construction loading method, which consists of 34 vertical columns with a width of 20 cm and a height of 5 m. Details of this loading method will be described next.

4.2. Initial condition and boundary conditions

In this model, the initial condition consists of 2 states: a) pore water pressure and b) the initial stress and geometry configuration. In the first state, the water level of the soil mass was assumed to be between the "base soil" and "soil" sections (see Figure 3). For defining the initial stress and geometry configuration, the vertical loading columns and metal shell were assumed to be inactive. Next, through the "generate initial stresses" option, the value of K_0 was defined for the soil mass.

According to Figure 3, the base line of the "base soil" was fixed in both the horizontal and vertical directions. Furthermore, all of the vertical lines of the "soil" section and vertical loading columns were fixed in a horizontal direction.

4.3. Imported numerical quantities for the soil–steel structure

The constitutive model of the "base soil" was assumed to be the Mohr–Coulomb, whose parameters were defined as $E_s = 130$ MPa, $\gamma_d = 19$ kN/m^3, $\gamma_\omega = 21.5$ kN/m^3, $\upsilon_s = 0.15$, c = 10 MPa, $\varphi = 32^\circ$, and $\psi = 0^\circ$. These parameters were fixed throughout the modeling procedure.

The main part of this study is the examination of the effect of soil property variations on the stability of the soil–steel culvert. The constitutive model used for the "soil" section of the model was assumed to be Mohr–Coulomb. The imported numerical values for this part of the model and their effects on the behavior of the soil–steel culvert will be discussed later.

For the corrugated metal plates, according to El-Sawy (2003), the properties of an equivalent plate section were used. As mentioned above, the equivalent Young's modulus $\bar{E}$= 23080 MPa and equivalent plate thickness $\bar{t}$= 6.1 mm were defined for the model. Other characteristics of the metal shell per unit length of the corrugated plate are:

A = 0.0061 m^2; I = 1.89E-8 m^4; w = 0.478 kN/m; $\upsilon = 0.3$

4.4. Stage construction loading method

According to studies performed by El-Sawy (2003), the values and positions of the applied loadings are shown in Figure 4. A 5-axes truck was modeled for that program. Figure 4 shows the plan and front view of the axes and applied loads on each axis. In PLAXIS, only 2 extended loads can simultaneously be defined for a model, so 2 backward axes with maximum loads (147.6 kN) were chosen. The loading area of each axis was assumed to be 20 cm; hence, on the "soil" surface of the culvert, 34 columns with a width of 20 cm and a height of 5 m were modeled (see Figure 3). Therefore, the loading procedure could be done by applying the given γ_d values for these columns as overburden. The distance between 2 axes was assumed to be 1.8 m; hence, in the stage construction method, in each loading phase, 2 columns with a distance of 1.8 m (or 9 columns) were chosen. In the 1st phase, for example, the 1st and 10th columns became active (were defined γ_d values) and other columns became inactive. In the 2nd phase, the 2nd and 11th columns became active and other columns became inactive and so on. Finally, 25 loading phases were defined for the model.

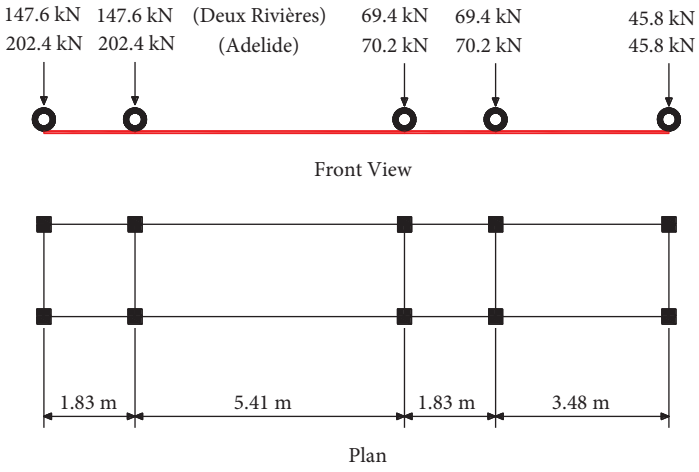

Figure 4. Plan and front view of the axes and applied loads on each axis (taken from El-Sawy (2003)).

Because the soil columns of loading were defined only for the loading purpose, it is important to note that high height, low width, and relatively high γ_d values for these columns could cause condensation and collapse

in their configuration (the height is 25 times more than the width). Therefore, a value of E_{steel} was defined for these columns that had no effect on the program results.

5. Modeling results and discussion

In this section, the effect of the soil property variations on the stability of the soil–steel culvert is discussed.

5.1. Effect of cohesion (c) variations on stability of the soil–steel culvert

At first, initial values of the "soil" mass E = 60 MPa, $\upsilon = 0.25$, $\gamma_\omega = 19$ kN/m^3, $\gamma_d = 17.5$ kN/m^3, $\varphi = 30^\circ$, $\psi = 2^\circ$, and c = 10 MPa were defined for the model. Next, stage construction loading was applied to the model. Analyses showed that the soil–steel culvert collapsed in phase 4 of the loading, until an increasing of the c values up to 14 MPa. With c = 15 MPa, the soil–steel culvert collapsed in phase 17 of the loading, and by increasing c values, the culvert could bear the applied loading until the final loading phase.

According to Figure 3, from the 9th to the 16th phase, the forward load axis passes from the culvert crown and enters the "unloading" state, whereas the backward load axis exists before the culvert crown, and by approaching the crown, the thrust force induced by the backward axis increases. This state can be named the "intermediate" state. From the 17th loading phase to the final phase, both axes have passed from the culvert crown, and this state can be named the "unloading" state.

5.1.1. Interpretation of c values' variation

According to the results, the model failure in the 4th loading phase at c = 10–14 MPa can be explained as a result of the lack of cohesion strength in the "soil" mass. In the case of c = 15 MPa and its consequence failure in the 17th loading phase, the failure of the soil–steel culvert can be stated as a result of the residual stress on the "soil" mass due to the "unloading" process. Figure 5 shows that as the amount of cohesion values in the "soil" mass increases, the bearable load of the soil–steel culvert increases.

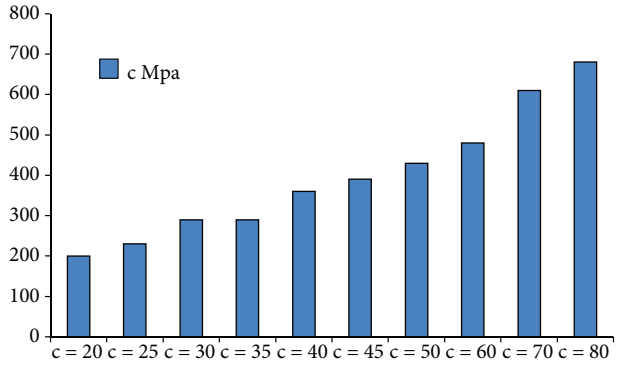

Figure 5. Maximum bearable load of the soil–steel culvert (MPa) vs. the cohesion values (MPa).

The results explain that the cohesion parameter in the "soil" mass can be an important factor in increasing the bearing capacity and stability of the soil–steel culvert. Furthermore, cohesion plays an undeniable role in control of the residual stress effects on the soil–steel culvert stability induced by the "unloading" state.

5.2. Effect of Young's modulus (E) variations on the stability of the soil–steel culvert

Young's modulus (E) is one of the Mohr–Coulomb parameters needed for the numerical model. To examine the variations of this parameter on the soil–steel culvert behavior, several parametric studies were carried out. For this aim, the "soil" mass was defined with these properties for the model: $\upsilon = 0.25$, $\gamma_\omega = 19$ kN/m^3, $\gamma_d = 17.5$ kN/m^3, $\varphi = 30^\circ$, and $\psi = 2^\circ$. Three various cohesion values equal to 14, 16, and 20 MPa were also defined for the model. Using 3 different axis load values for the model, the effect of the Young's modulus (E) variations on the stability of the soil–steel culvert was examined.

5.2.1. Effect of Young's modulus variations on the thrust force and residual stress induced by the applied loading

Considering Table 2, models with E = 30–60 MPa could not bear the applied loading and the soil–steel culvert collapsed in the 4th phase. The 5th model (E = 70 MPa) also collapsed in the 9th phase of the loading process and the 6th model (E = 80 MPa) collapsed in the 17th phase of the loading process, whereas the 7th model (E = 90 MPa) could bear all of the loading phases.

Table 2. Numerical modeling results for c = 14 MPa and applied loading equal to 150 kN.

E (MPa)	Load (kN)	Calculation state	Maximum displacement on the soil surface (mm)	Maximum displacement on shell crown (mm)
30	150	Failed in phase 4	-	-
40	150	Failed in phase 4	-	-
50	150	Failed in phase 4	-	-
60	150	Failed in phase 4	-	-
70	150	Failed in phase 9	-	-
80	150	Failed in phase 17	-	-
90	150	Fully reached	18.32	29

It can be explained that the first 4 models collapsed as a result of an increase in the thrust force and its consequence in the soil displacements and deformations. The soil–steel culvert in the 5th model collapsed in the "intermediate" state of the loading process, and in the 6th model, the soil–steel culvert collapsed as a result of the "unloading" process, which caused residual stresses in the "soil" mass.

According to results shown in Tables 3 and 4, increasing both the E and c values causes an increase in the bearing capacity and stability of the soil–steel culvert. As with the c values, increasing the E values increased the residual strength of the "soil" mass under the "unloading" condition.

5.2.2. Effect of Young's modulus variations on the stability and deformations of the culvert induced by the applied loading

Considering Table 4, it can be concluded that the "soil" mass and culvert crown displacements are due to the applied loading. Figure 6 summarizes these results.

According to Figure 6, increasing the E values causes a reduction in both the soil surface and the culvert crown displacements. As the "compaction literature" explains, increasing the compaction energy can cause an increase in Young's modulus, which causes less deformation under the applied loading. Because the "soil" mass

has an interaction with the metal shell of the culvert, higher E values can lead to a decrease in the culvert crown displacements and an increase in the stability of the soil–steel structure.

Table 3. Numerical modeling results for c = 16 MPa and applied loading equal to 170 kN.

E (MPa)	Load (kN)	Calculation state	Maximum displacement on the soil surface (mm)	Maximum displacement on shell crown (mm)
30	170	Failed in phase 4	-	-
40	170	Failed in phase 4	-	-
50	170	Failed in phase 15	-	-
60	170	Fully reached	28.28	37
70	170	Fully reached	26.05	35
80	170	Fully reached	22.95	33
90	170	Fully reached	22.06	32

Table 4. Numerical modeling results for c = 20 MPa and applied loading equal to 190 kN.

E (MPa)	Load (kN)	Calculation state	Maximum displacement on the soil surface (mm)	Maximum displacement on shell crown (mm)
30	190	Fully reached	52.74	56
40	190	Fully reached	46.22	48
50	190	Fully reached	34.28	43
60	190	Fully reached	31.65	39
70	190	Fully reached	28.22	37
80	190	Fully reached	24.57	35
90	190	Fully reached	22.88	34

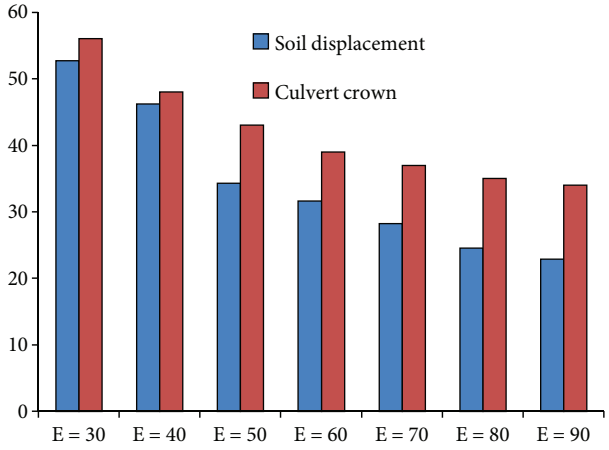

Figure 6. Maximum displacements of the "soil" mass (mm) and culvert crown (mm) vs. the variations of E values (MPa).

5.3. Effect of friction angle (φ) variations on stability of the soil–steel culvert

As the internal friction angle plays an important role in the shear strength of a soil mass, variations of this parameter were considered in this paper. According to Table 1, the range of φ values was assumed to be from

26° to 40° with a 2° increment. Two states were considered for this part of the parametric model: the 1st state, with E = 70 MPa, c = 15 MPa, and an applied load of 147.6 kN, and the 2nd state, with E = 70 MPa, c = 18 MPa, and an applied load of 160 kN.

5.3.1. Interpretation of the φ values' variation

In the first state, with $\varphi = 26°$ and $\varphi = 28°$, and in the second state, with $\varphi = 26°$ and $\varphi = 27°$, the soil–steel culvert collapsed in the 4th loading phase. This means that the culvert could not bear the thrust force in the "loading" state. In the first state, with $\varphi = 29°$, the soil–steel culvert collapsed in the 9th loading phase due to residual stresses.

According to the difference between the results obtained in the states with $\varphi = 26°$ and $\varphi = 30°$ from Table 5 and $\varphi = 26°$ and $\varphi = 28°$ from Table 6, the internal friction angle (φ) is a parameter whose high values can lead to an increase in the soil–steel culvert strength regarding the applied loading and trust forces. Tables 5 and 6 demonstrate that as the internal friction angle (φ) increases, the displacements of the soil surface decrease. Therefore, an increase in the internal friction angle (φ) can cause the soil–steel culvert to be more stable, whereas this increase has a negligible effect on the metal crown displacements.

Table 5. Numerical modeling results for c = 15 MPa and applied loading equal to 147.6 kN.

φ (degrees)	Load (kN)	Calculation state	Maximum displacement on the soil surface (mm)	Maximum displacement on shell crown (mm)
26	147.6	Failed in phase 4	-	-
28	147.6	Failed in phase 4	-	-
29	147.6	Failed in phase 9	-	-
30	147.6	Fully reached	23.75	30
32	147.6	Fully reached	21.38	30
34	147.6	Fully reached	20.51	29
36	147.6	Fully reached	19.80	29
38	147.6	Fully reached	18.10	28
40	147.6	Fully reached	17.35	28

Table 6. Numerical modeling results for c = 18 MPa and applied loading equal to 160 kN.

φ (degrees)	Load (kN)	Calculation state	Maximum displacement on the soil surface (mm)	Maximum displacement on shell crown (mm)
26	160	Failed in phase 4	-	-
27	160	Failed in phase 4	-	-
28	160	Fully reached	23.80	32
30	160	Fully reached	23.51	31
32	160	Fully reached	22.38	31
34	160	Fully reached	21.64	31
36	160	Fully reached	20.59	30
38	160	Fully reached	18.53	30
40	160	Fully reached	18.04	29

5.4. Effect of other parameter variations on the stability of the soil–steel culvert

5.4.1. Variations of Poisson's ratio (υ)

Table 7 shows the results of Poisson's ratio variations in the "soil" mass. In this state, for the "soil" mass, these properties are E = 70 MPa, γ_ω = 19 kN/m^3, γ_d = 17.5 kN/m^3, c = 20 MPa, $\varphi = 20^\circ$, and $\psi = 2^\circ$, and the applied loading on 2 axes is 147.6 kN.

Table 7. Numerical modeling results for various υ values.

υ	Load (kN)	Calculation state	Maximum displacement on the soil surface (mm)	Maximum displacement on shell crown (mm)
0.2	147.6	Fully reached	21.38	28
0.25	147.6	Fully reached	20.83	28
0.3	147.6	Fully reached	19.20	28
0.35	147.6	Fully reached	19.12	27
0.4	147.6	Failed in phase 9	-	-

According to the results of Table 7, variations in the υ values cause a negligible reduction in the deformation in both the soil surface and the shell crown, and in the state with $\upsilon = 0.4$, the soil–steel culvert collapsed. This result might be due to an increase in the soil plasticity.

5.4.2. Variations of the dilation angle (ψ)

The dilation angle (ψ) always has small values. Considering that E = 70 MPa, γ_ω = 19 kN/m^3, γ_d = 17.5 kN/m^3, c = 20 MPa, $\varphi = 20^\circ$, $\upsilon = 0.25$, $\varphi = 30^\circ$, and the applied loading on 2 axes is 147.6 kN, the results of the parametric study are shown in Table 8.

Table 8. Numerical modeling results for various ψ values.

ψ (degrees)	Load (kN)	Calculation state	Maximum displacement on the soil surface (mm)	Maximum displacement on shell crown (mm)
0	147.6	Fully reached	21.78	28
1	147.6	Fully reached	21.50	28
2	147.6	Fully reached	20.83	28
3	147.6	Fully reached	20.62	28

As with Poisson's ratio, variations in the ψ values cause a negligible reduction in the deformation of the soil surface and no deformation in the shell crown. Therefore, it can be concluded that an increase of the dilation angle values has no effect on the stability of the soil–steel culvert.

6. Summary and conclusions

1. Increasing the values of cohesion (c) leads to an increase of the culvert's strength; thus, the soil–steel culvert can bear the thrust forces due to the "loading" process and the residual stresses due to the "intermediate loading" and "unloading" processes.
2. Young's modulus plays an important role in the stability of the soil–steel culvert. As E values increase, the "soil" mass strength increases and the soil–steel culvert can bear the thrust forces due to the "loading"

process and the residual stresses due to the "unloading" process. Furthermore, the higher the E values, the lower the displacements in both the soil surface and the shell crown; hence, the stability of the soil–steel culvert increases.

3. Increasing the internal friction angle (φ) can slightly reduce the failure of the soil–steel structure as a result of the thrust forces in the "loading" state. Furthermore, the effect of the increasing φ values on the increase in the soil strength regarding the residual stresses in the "unloading" state is negligible. Moreover, increasing the φ values has a minor effect on the stability and stiffness of the metal shell.
4. As Poisson's ratio (υ) increases, the plastic index of the soil mass increases and the stability of the soil mass regarding the loading slightly decreases.
5. The dilation angle (ψ), according to its lowest values in all kinds of soils, has a negligible effect on the stability of a soil–steel culvert.

References

AASHTO, American Association of State Highway and Transportation Officials, Standard Specifications for Highway Bridges, Washington DC, 1989.

Bakht, B., "Soil-Steel Structure Response to Live Loads", Journal of Geotechnical Engineering Division ASCE 107, 779–798, 1981.

Barkhordari, M.A. and Abdel-Sayed, G., "The Parameters Controlling the Strength of Soil-Steel Structures", International Journal of Engineering Science 12, 77–86, 2001.

Byrne, P.M., Srithar, T. and Kern, C.B., "Field Measurements and Analysis of a Large-Diameter Flexible Culvert", Canadian Geotechnical Journal 30, 135–145, 1993.

El-Sawy, K.M., "Three-Dimensional Modeling of Soil-Steel Culverts under the Effect of Truckloads", Journal of Thin-Walled Structures 41, 747–768, 2003.

Girges, Y. and Abdel-Sayed, G., "Three-Dimensional Analysis of Soil-Steel Bridges", Canadian Journal of Civil Engineering 22, 1155–1163, 1995.

Kunecki, B., "Full Scale Tests of Corrugated Steel Culvert and FEM Analysis with Various Static Systems", Studia Geotechnicaet Mechanica 28, 39–53, 2006.

Machelski, C. and Antoniszyn, G., "Load Rate of the Circumferential Sector of Soil-Steel Bridge Structures", Archives of Civil and Mechanical Engineering 5, 85–102, 2005.

Moore, I.D. and Brachman, R.W.I., "Three-Dimensional Analysis of Flexible Circular Culverts", Journal of Geotechnical Engineering 120, 1829–1844, 1994.

PLAXIS, Version 8, Material Models Manual, PLAXIS b.v., Delft, the Netherlands, 2002.

Seed, R.B. and Raines, J.R., "Failure of Flexible Long-Span Culverts under Exceptional Live Load", Transportation Research Report No. 1191. Transportation Research Board, Washington DC, 22–29, 1988.

Taleb, B. and Moore, I.D., "Metal Culvert Response to Earth Loading Performance of Two-Dimensional Analysis", Transportation Research Report No. 1656, Transportation Research Board, Washington DC, 25–36, 1999.